Single- and multi-layered porous titanium via metal injection moulding

Mohammed Menhal Shbeh[1,2*], Russell Goodall[1]

[1]*Department of Materials Science and Engineering, University of Sheffield, Sir Robert Hadfield Building, Mappin Street, Sheffield S1 3JD, UK*
[2]*Department of Production Engineering and Metallurgy, University of Technology, Al-Sinaa' Street, 10066, Baghdad, Iraq*

[*]Corresponding author, Tel: (+44) 7459568184 ; E-mail: mmmshbeh1@sheffield.ac.uk

Received: 01 September 2016, Revised: 19 October 2016 and Accepted: 13 October 2016

DOI: 10.5185/amlett.2017.7052
www.vbripress.com/aml

Abstract

Titanium foams are advanced materials with macroporous structure that have a great potential in a variety of areas such as biomedical and functional applications. They are characterized by their reduced density and stiffness, with high permeability and excellent biocompatibility. One production technique for Ti foams with promising results is Metal Injection Moulding (MIM). So far most of the porous titanium produced by this technique has a very basic design with low percentage of porosity, thus limiting its potential in the biomedical industry, among others. In this study, the use of MIM in combination with a space holder to produce single and multi-layered porous Ti with high volume percentage of porosity will be explored. The results show that it is possible to produce Ti foam with a total volume percentage of porosity of 61 % through MIM technology. In addition, it is also feasible to combine different porous layers resulting in multi-layered porous titanium parts with gradient porosity that could have a huge potential in a wide range of applications, especially for biomedical implants, where these pores can promote bone ingrowth as well as reduce stiffness to match that of the natural bone, thus alleviating the stress shielding problem. Copyright © 2017 VBRI Press.

Keywords: Titanium foam, metal injection moulding, porous metal, space holder, micro-CT.

Introduction

Titanium foams are meso and macro porous structured materials with tailorable mechanical and acoustic properties depending on the amount of porosity in their structure. This character gives these advanced materials an advantage over other traditional materials, potentially matching their properties to optimally suit a variety of structural and functional applications in different working environments. One of the areas of greatest potential for such unique materials is in biomedical implants, where they can be used for replacing or treating large bone defects that result from severe fracture. These foams do not only offer the possibility to match the properties of the bone and mimic its structure, but also can reduce the risk of infection and donor site morbidity, compared to autografts **[1]**. Although Ti foams have previously been produced successfully with a good percentage of porosity, there are still challenges in making them with a complex structure that mimics the properties of the bone, for example by having compact outer layer surrounding more spongy layers.

There are many manufacturing methods for such unique materials, for example some based on powder metallurgical routes such as slip casting **[2, 3]**, impregnation of polymer foam **[4]**, freeze casting **[5]**, space holder technique **[6-9]** as well as gel casting **[10]**. One promising manufacturing technique is Metal Injection Moulding in combination with a Space Holder (MIM-SH). This technique does not only offer the possibility to mass produce these foams, but also near net shape them with minimized finishing operations and reduced cost. The process involves the injection of a homogenized mixture of metal powder, space holder and polymeric binder through a nozzle into a die with the desired product shape before removal of space holder and binder and sintering the part. So far most of the foams that have been reported to be produced by this technique have a relatively low percentage of porosity compared to other techniques such as the space holder (i.e. press and sinter). For instance, Morelli et al investigated the use of MIM-SH and produced Ti foams with a total porosity of up to 43% by adding 50% space holder **[11]**. Another study has used a modified MIM-SH process to produce Ti foams with 57% porosity by warm compacting a Ti feedstock with 70%vol. space holder, though the modified process resembles more the space holder technique rather than injection moulding, where a feedstock flows through a nozzle into a die **[12]**. The reason behind such a low porosity compared to other techniques, such as the space holder methods, lies in the fact that there are restrictions in terms of the maximum permissible amount and size of

space holder that can be added without sample collapse during debinding and sintering. For example, Tuncer et al explored the use of KCl to produce Ti foams and found that any space holder content higher than 55% leads to sample collapse **[13]**. Laptev et al reported that this limitation could be lifted through the sublimation of the KCl during sintering and produced Ti foams with a maximum porosity of 61.6% by adding 70% KCl to the feedstock **[14]**. However, sublimation of space holder can result in contamination of foams and furnace with KCl and can result in undesirable phases which can be quite detrimental. In addition to the low porosity challenge, most of the foams reported in the literature by this technique have a very basic design which does not manifest the main advantage of MIM technology in processing complex shapes. In this paper, the use of MIM-SH to produce single layered Ti foams with high volume percentage of porosity and complex design will be explored. The foams produced have a novel, radially graded porous structure, which allows more complex behaviours, potentially closer to those of bone. In addition, the ability to combine microporous and macroporous injection moulded layers along the height of the cylinder will be investigated. This is a little-explored area, yet is of great importance as components making use of porous titanium are likely to also require dense regions (e.g. for strength) and the bond between the two is critical.

Experimental

Preparation and characterization of single layered Ti foam

Commercially pure Ti powder grade 2 (Arcam AB, Sweden) with a mean particle size of 74.9 µm was used in this study and mixed with a polymeric binder and space holder. The binder was composed of Polyethylene glycol 1500, Poly methyl methacrylate (PMMA) and stearic acid. The space holder used was spherical potassium chloride with a mean particle size of 319 µm. The solid loading was about 58 %vol. of which 60% was KCl and the rest was Ti. The mixture of the powders and binder were mixed using a high speed centrifugal mixer with four milling media in similar manner to our previous study **[15]**. The mixture was then extruded twice at 150 ºC using a low pressure injection moulder with a maximum pressure of 45 MPa and pelleted into small pellets before injecting cylindrical samples with a 10mm diameter and approximately 13 mm in height. A schematic of the MIM-SH process is shown in **Fig. 1. (a)**. The samples were then debound ultrasonically at a temperature of 50 ºC for quicker space holder and PEG removal, based on the findings of our previous study, and subsequently dried in order to remove any moisture. Next, the samples were thermally debound at 450 ºC for 1h in order to remove the PMMA and sintered in a vacuum furnace (Centorr, USA) at 1250 ºC for 2h. In order investigate the suitability of the process for complex parts, an attempt was made to produce porous surgical staples by injecting a feedstock with 35% KCl into a barbed staple mould and the injected parts were then debound and sintered using the same parameters as the single layer foams. The KCl used for the medical staples was cubic with a mean particle size of 348 µm. For comparison, some medical staples were injection moulded using a feedstock with similar solid loading, but without space holder. The percentage of porosity for the single layer foams was calculated by estimating the real volume of the foam through a helium pycnometer and subtracting it from the bulk volume and the value was compared with the porosity percentage estimated by the Micro-CT analysis. Volume shrinkage of samples was monitored using a calliper with a resolution of 0.01 mm. The foams produced were characterized using a SkyScan1172 Bruker Micro-computed tomography system with a voxel size of 6 µm using 1mm Al filter. For ease of data analysis, a 4 mm section of the foam was analysed in 3D and a threshold value of 70 was used. In addition, the foams produced were mechanically tested under compression loading using Zwick Z050 machine at a strain rate of 0.001 s^{-1} according to ISO 13314.

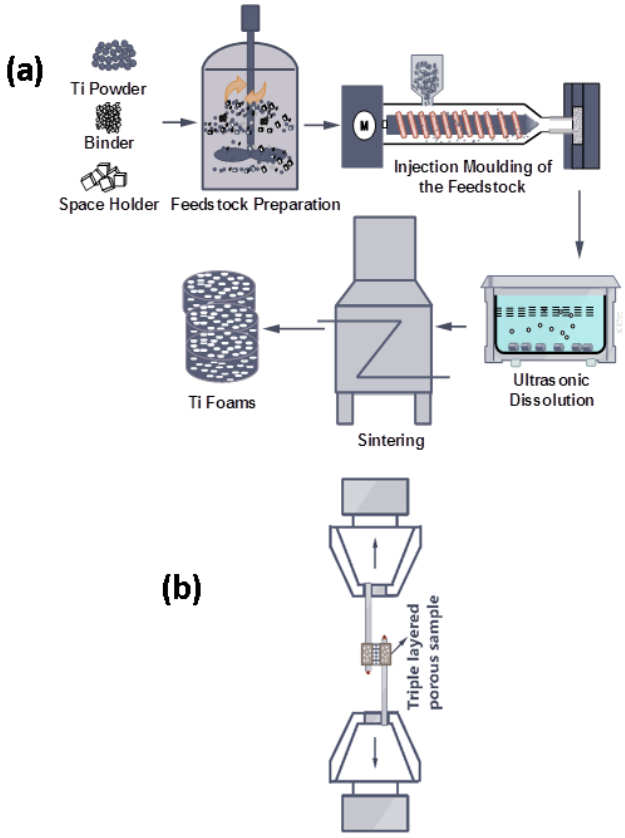

Fig. 1. (a) Schematic of MIM-SH process, (b) shear testing assembly.

Preparation and characterization of multi - layered porous Ti

The preparation of multi-layered porous Ti was attempted by injecting two different feedstocks into the same mould at different intervals. The first feedstock was prepared using the same Ti powder with a solid content of 58% and 0% KCl, while the second feedstock had 58% solid content of which 60% was KCl. The KCl used was cubic

Copyright © 2017 VBRI Press

with a mean particle size of 348 µm. The process was designed so that the samples have three porous layers, two microporous layers with one macroporous layer positioned at the centre of the samples. Another attempt was carried out by injecting one microporous layer with one macroporous layer. The main source of pores for the microporous layers are the micropores that result from partial bonding and incomplete neck formation among the Ti particles during sintering. Shear testing for the triple porous layers was performed using two specially developed holders that enable holding the samples from the microporous layers, thus ensuring much of the shearing load is localised at the macroporous layer. The testing assembly is shown in **Fig.1. (b)**.

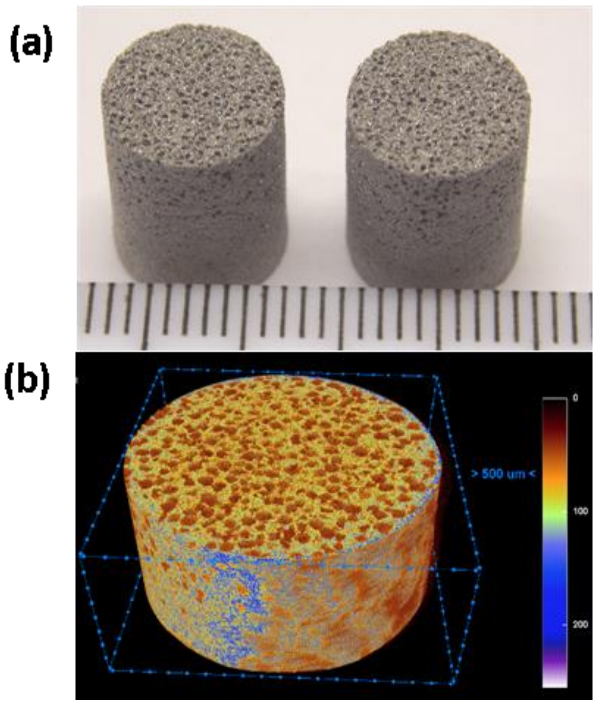

Fig. 2. (a) Single layered porous Titanium, (b) Volume rendered model of a 4mm section of a foam produced. The colour spectrum indicates density, with dark red being lowest density and blue the highest.

Results and discussion

Fig. 2 shows the single layered Ti foams produced by the MIM-SH process with a 3D volume rendered 4mm section of a foam produced. The results of the porosity analysis based on the pycnometry measurements showed that the foams produced had a total percentage porosity of about 61.25%±0.29, whereas the results of the 3D analysis of the micro CT showed that the foam had a total percentage porosity of about 61.5% of which 0.18% is closed porosity. Hence, both measurement methods showed approximately similar results and are in a good agreement, if a lower grey threshold value of 70 is applied for micro CT, as this value dictates the appearance of each voxel in the scanned data. Any voxel with grey value higher than 70 will appear as solid, whereas lower value voxels will be background. The volume shrinkage of samples after sintering was 34.45%± 0.84.

It should be noted that the volume percentage of porosity achieved is approximately equal to the volume percentage of porosity obtained in the study of Laptev *et al*. **[14]**, even though the volume percentage of space holder added in their study was much higher than that in the current study; their solid content was about 70 of which 70% was KCl. This can be attributed to several factors such as the relatively coarse Ti powder used in this study, the higher volume percentage of binder used as well as the wider particle size distribution of the KCl used in this study as the KCl powder used here had a particle size ranging from 127-516 µm. The wider the particle size distribution, the better the interconnectivity of the pores as smaller KCl particles can sit among larger particles providing a better and closer packing of pores.

Table 1. Some characteristic parameters obtained via CT analysis.

Parameter	Value
Total volume of a 4mm section (mm^3)	248
Object or solid volume (mm^3)	95.60
Surface area of the Total Volume (mm^2)	254
Surface area of solid object (mm^2)	5790
Surface area of closed pores (mm^2)	40.20

It was also observed that the foams produced had a denser outer layer with a much lower amount of macropores compared to the centre of the sample. This is expected due to the fact that the KCl particles cannot get closer to the surface than when they were touching the mould. This observation can be clearly seen in the volume rendered CT section, where the colour bar is indicative of the density difference between different regions in the foam. The blue colour refers to the highest density part of the foam, while the dark red colour refers the lowest. This density difference is quite beneficial, particularly for biomedical applications as this structure mimics the structure of the bone, where the outer layer provides strength and structural integrity in a similar manner to the outer layer of the natural bone, whereas the inner spongy layer consists of micro and macro porous channels, that enable bone ingrowth, nutrient exchange as well as cell migration and attachment **[16]**. **Table 1** shows some important parameters for the 4mm section of the foam produced which were obtained via the micro CT analysis. As seen from the data, the surface area of all the solid objects within the volume is more than 22 times higher than the surface area of the volume scanned (i.e. the area of the cylinder-like section) showing the much greater internal surface area that these foams have because of their porosity with great potential for biomedical applications.

Pore size analysis for the foam produced was carried out using CTAn analyzing software in 3D. The results of the pore size analysis are shown in **Fig. 3. (a)**. It can be clearly seen that there are two distinctive regions in the curve, one with much more narrow Gaussian distribution and it starts with 6 µm and it extends up to 67 µm, reflecting the size of the micropores that result from incomplete sintering of the Ti particles. The second region has a much wider Gaussian distribution with larger

Copyright © 2017 VBRI Press

sizes of pores up to 481 µm which reflects the broad range of the KCl particle size distribution that was used in this study. It is important to point out that there is a transitional region that connects the microporous region with the narrow Gaussian distribution from the KCl induced macroporous region with the wide Gaussian distribution, and the pores in this third region range from 67-150 µm. Hence, the foams produced have a very wide pore size distribution with high interconnectivity that resemble the natural cancellous bone structure, where the pores in cancellous bone vary in sizes and can reach up to 470 µm **[17**, **18]**. Having this broad pore size distribution is also important for osteoconductivity as it has been reported that for the metal foam to be osteoconductive, it must have pore sizes in the range of 100-500 µm **[19]**.

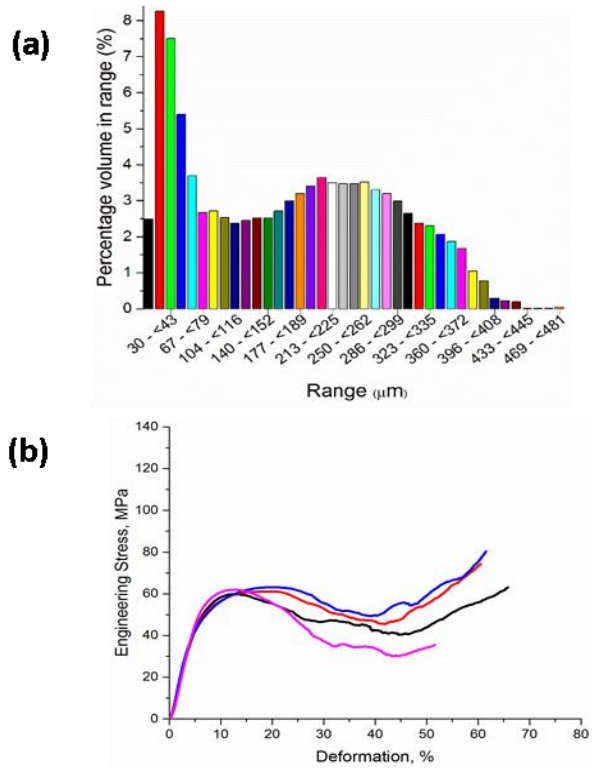

Fig. 3. (a) Pore size range versus the amount in that range, (b) Compression testing results for four foams.

The foams produced had a yield stress of 36.7±3.4 MPa and elastic modulus of about 1.1 ±0.7 GPa. The results of the compression test for four foams produced are shown in **Fig. 3. (b)** and **Fig. 4**. These values are relatively close to the mechanical properties of the cancellous bone, where it has a yield strength of 25.0±8.1 MPa and elastic modulus value of 1.08±0.86 GPa **[20**, **21]**. Taniguchi *et al.* has recently produced and mechanically tested porous titanium parts with 61.6%±0.4 porosity and 80% of these pores were ranging in size between 240-420 µm by Selective Laser Melting (SLM) **[22]**. They reported an elastic modulus value of 0.557 GPa and compressive yield strength of 36.2 MPa. Thus, one could argue that foams produced by the current study have relatively higher mechanical properties compared to these previous foams, achieved with approximately similar volume percentage of pores, of course noting that our stochastic structure and their regular lattice structure are different and their foams were heat treated after SLM for 1 h at 1300 ºC. It is also important to point out that the powder used in this study is relatively coarser than a typical SLM powder and that normally used for Electron Beam Melting (EBM); using a finer powder would result in improved mechanical properties.

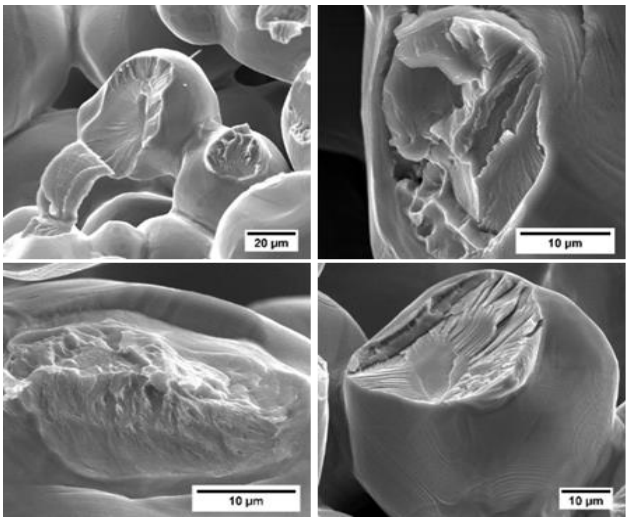

Fig. 4. Fracture surface of the Ti particles.

It was observed from the SEM analysis that failure mostly occurs at the incomplete necks among the bonded Ti particles with some cases of broken Ti particles.

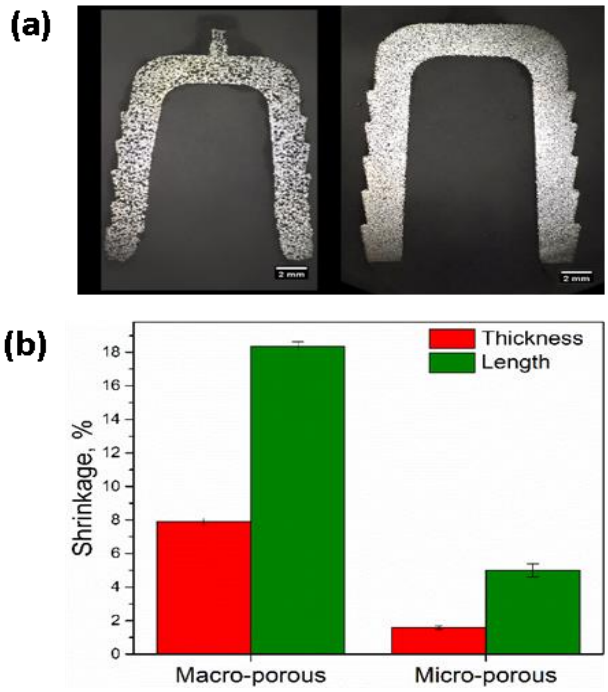

Fig. 5. (a) Micro and macroporous medical staples, (b) Dimensional changes of medical staples after sintering.

In addition, there were also some micro-dimples at the surface of the broken particles indicating some ductile

Copyright © 2017 VBRI Press

character to the failure. However, failure at particles showed striated structure. The result of the injection process of the medical staple is shown in **Fig. 5**.

It can be seen from **Fig. 5** that the porous barbed staple retained its shape to some degree even though it shrank significantly. However, the interconnected pores formed crack-like paths at the edges of the staple, thus it is expected to have much inferior mechanical properties compared to the microporous ones made without space holder.

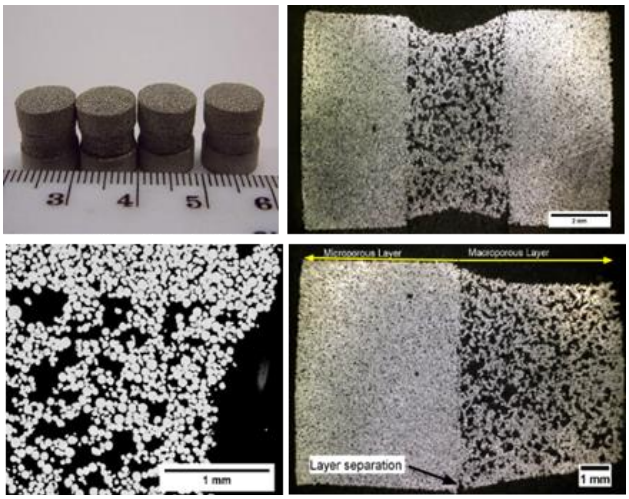

Fig. 6. Double and triple layered porous Ti.

The result of the multi-layer trial is shown in **Fig. 6**. It can be observed from **Fig. 6** that there is good bonding between the macroporous and the microporous layers as we move away from the outside edges towards the centre of the samples. However, layer separation was noted at some edges of the interface between the macro and micro porous layers. This layer separation was found to be initiated during debinding and the depth of separation was ranging from 300 µm up to 1 mm. This layer separation can be attributed to two main factors, namely, the differences in the volume shrinkage between the porous and dense part during debinding and the time interval of injection between each shot or layer due to equipment limitation. As each layer was injected with time difference of about 10-15 minutes which was required to empty the barrel from the feedstock with no space holder and load it with a feedstock that has 35% KCl. This resulted in poorer bonding at the green body stage than would be achieved if injection were sequential with no delay. This could be solved with the use of two component injection moulding or low pressure injection system with multiple barrels. It was also noticed that some KCl particles have infiltrated the bottom microporous layer in both attempts, which could be due to left over feedstock with KCl in the nozzle or barrel. In addition, the foam or the macroporous layer in the triple layered porous samples took a neck-like shape, where the microporous layers confined the movement of the particles at the interface during sintering leaving the centre of the foam to shrink freely resulting in a neck-like shape. Thus, it is expected that high residual stresses may be concentrated at the interface which might lead to failure at an early stage. This was confirmed by the shear test results for the triple layered porous samples as shown in **Fig. 7**.

All the samples failed at the interface between the macro and micro porous layers as expected. Nevertheless, some bits of the macroporous layer were still intact and bonded to the microporous layers even after fracture indicating the presence of good bonding in some areas among the microporous and macroporous layers. It was also observed that mainly necks were broken with few Ti particles with similar striated structure to that observed for the compression testing of single layered porous Ti. This might suggest that crack propagation follows the weakest bonds or necks between the bonded Ti particles.

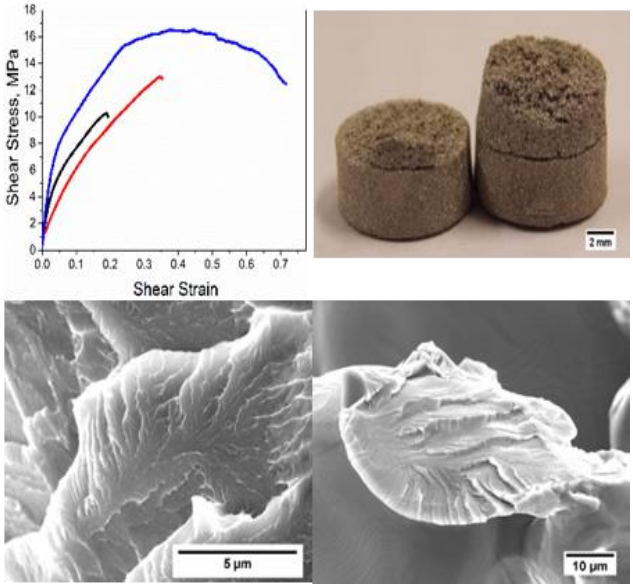

Fig. 7. Shear testing results of three samples and fracture surface of the triple layered porous titanium.

Conclusion

Ti foams are advanced materials with micro and macroporous structure that have many potential applications in different areas. Single layered porous Ti foams with a total volume percentage of porosity of about 61% (of which 99.7 % is open pores) have been produced in this study. The foams produced had a yield stress of about 60MPa and elastic modulus of about 1.1 GPa which are quite close to the mechanical properties of cancellous bone, indicating the great potential of such foams in biomedical applications. The surface area of the solid making up the foam was 22 times that of a solid shape of the same volume. Macroporous barbed biomedical staples with relatively complex shape have also been manufactured in this study, indicating the great potential of MIM in processing porous parts with complex geometries. However, shrinkage could be an issue which might require modifications to the design of the part in order to be overcome. In addition, double and triple layered porous titanium with macro and micro porous

Copyright © 2017 VBRI Press

layers have been produced successfully through MIM-SH process. However, some layer separation occurs at the interface during debinding and this has led to sample failure at low shear stress during shear testing at the interface. Nonetheless, some parts of the macroporous layer were still bonded with the microporous layer even after fracture. This problem could be overcome through the use of a low-pressure injection moulding system with multi barrel system, as in a biomedical implant confidence in the bond across interfaces must be high.

Acknowledgements

One of the authors (MMS) would like to acknowledge a studentship from the Iraqi Ministry of Higher Education and Scientific Research. We would also like to thank Ms Evi Bongaers for the useful discussion about 3D analysis.

Author's contributions

Mohammed Shbeh conceived the plan, performed the expeirments and wrote the paper and all done under supervison of the second author Dr. Russell Goodall. Authors have no competing financial interests.

References

1. Kartus, J.; Movin, T.; Karlsson, J.; Arthroscopy, **2001**, 17 (9), 971. **DOI:** 10.1053/jars.2001.28979
2. Neirinck, B.; Mattheys, T.; Braem, A.; Fransaer, J.; Van der Biest, O.; Vleugels J.; Adv Eng Mater., **2009**, 11 (8), 633. **DOI:** 10.1002/adem.200900074
3. Xu, Q.; Gabbitas, B.; Matthews, S.; Zhang, DL.; J Mater Process Tech., **2014**, 214 (3), 734. **DOI:** 10.1016/j.jmatprotec.2013.03.011
4. Cachinho, SCP.; Correia, RN.; Powder Technol**.,** **2007**, 178 (2), 109. **DOI:** 10.1016/j.powtec.2007.04.014
5. Li, JC.; Dunand, DC.; Acta Mater., **2011**, 59 (1), 146. **DOI:** 10.1016/j.actamat.2010.09.019
6. Jakubowicz, J.; Adamek, G.; Dewidar, M.; J Porous Mat., **2013**, 20 (5), 1137. **DOI:** 10.1007/s10934-013-9696-0
7. Mondal, DP.; Patel, M.; Das, S.; Jha, AK.; Jain, H.; Gupta, G.; Arya, S.B.; Mater Design., **2014**, 63, 89. **DOI:** 10.1016/j.matdes.2014.05.054
8. Smorygo, O.; Marukovich, A.; Mikutski, V.; Gokhale, AA.; Reddy, GJ.; Kumar, JV.; Mater Lett., **2012**, 83,17. **DOI:** 10.1016/j.matlet.2012.05.082
9. Ye, B.; Dunand, DC.; Mat Sci Eng a-Struct., **2010**, 528 (2), 691. **DOI:** 10.1016/j.msea.2010.09.054
10. Erk, KA.; Dunand, DC.; Shull, KR.; Acta Mater., **2008**, 56 (18), 5147. **DOI:** 10.1016/j.actamat.2008.06.035
11. Carreno-Morelli, E.; Rodriguez-Arbaizar, M.; Amherd, A.; Bidaux, JE.; Powder Metall., **2014**, 57 (2), 93. **DOI:** 10.1179/0032589914Z.000000000164
12. Barbosa, APC.; Bram, M.; Stöver, D.; Buchkremer, HP.; Adv Eng Mater., **2013**, 15 (6), 510. **DOI:** 10.1002/adem.201200289
13. Tuncer, N.; Bram, M.; Laptev, A.; Beck, T.; Moser, A.; Buchkremer, HP.; J Mater Process Tech., **2014**, 214 (7), 1352. **DOI:** 10.1016/j.jmatprotec.2014.02.016
14. Laptev, AM.; Daudt, NF.; Guillon, O.; Bram, M.; Adv Eng Mater., **2015**,17 (11), 1579. **DOI:** 10.1002/adem.201500061
15. Shbeh, MM.; Goodall, R.; Mater Design., **2015**, 87, 295. **DOI:** 10.1016/j.matdes.2015.08.018
16. Hannink, G.; Arts, JJC.; Injury., **2011**, 42, Supplement 2, S22 **DOI:** 10.1016/j.injury.2011.06.008
17. Dabrowski, B.; Swieszkowski, W.; Godlinski, D.; Kurzydlowski, KJ.; J Biomed Mater Res B., **2010,** 95B (1), 53. **DOI:** 10.1002/jbm.b.31682
18. Wang, XD.; Ni, QW.; J Orthopaed Res., **2003**, 21 (2), 312. **DOI:** 10.1016/S0736-0266(02)00157-2
19. Kohl, M.; Bram, M.; Buchkremer, HP.; Stover, D.; Habijan, T.; Koller, M. Medical Device Materials Iv., **2008**,14. **DOI:** 10.1361/cp2007mpmd014
20. Chen, L- J.; Li, T.; Li, Y-m.; He, H.; Hu, Y H..; Nonferr Metal Soc., **2009**, 19 (5), 1174. **DOI:** 10.1016/S1003-6326(08)60424-0
21. Shimko, DA.; Shimko, VF.; Sander, EA.; Dickson, KF.; Nauman, EA.; J Biomed Mater Res B., **2005**, 73B (2), 315. **DOI:** 10.1002/jbm.b.30229
22. Taniguchi, N.; Fujibayashi, S.; Takemoto, M.; Sasaki, K.; Otsuki, B.; Nakamura, T.; Mat Sci Eng C-Mater., **2016**, 59, 690. **DOI:** 10.1016/j.msec.2015.10.069